REVIEW ARTICLE

Establishing a Chest MRI Practice and its Clinical Applications: Our Insight and Protocols

Christine U. Lee, Darin B. White, Anne-Marie G. Sykes

Department of Radiology, Mayo Clinic, Rochester MN, USA

Address for correspondence:
Dr. Christine Lee,
Department of Radiology, Mayo Clinic,
200 Frist Street SW, Rochester MN
55905, USA.
E-mail: lee.christine@mayo.edu

ABSTRACT

Despite its nonionizing technique and exquisite soft tissue characterization, noncardiovascular, and nonmusculoskeletal magnetic resonance imaging (MRI) of the chest has been considered impractical due to various challenges such as respiratory motion, cardiac motion, vascular pulsatility, air susceptibility, and paucity of signal in the lung. With advances in MRI, it is now possible to perform diagnostically useful and good quality MRIs of the chest, but literature on subspecialized chest MRI practices is limited. The purpose of this manuscript is to describe the rationale, nuances, and logistics that went into developing such a practice in the Division of Thoracic Radiology at our institution. The topics addressed include technical and clinical considerations, support at administrative and clinical levels, protocol development, and economic considerations compared with conventional practices. Various MRI techniques are also specifically discussed to facilitate chest MRI at other sites. Although chest MRI is used in a relatively small number of patients at this point, in certain patients, chest MRI can provide additional information to optimize medical management. A few clinical cases illustrate the quality and clinical utility of chest MRI. Given recent advances in MRI techniques, it is now an opportune time to develop a chest MRI practice.

Key words: Chest magnetic resonance imaging, protocols, practice, thoracic MRI

INTRODUCTION

"Order an MRI of the chest? Can we do that?"
"I am not aware of any clinical indications for lung MR at this time."

"Medical training mantra (albeit more than 10 years ago) was to never order an MRI of the chest."
"How much does a chest MRI cost compared to a CT?"

These were some comments from many of our clinical and even radiology colleagues when our Division of Thoracic Radiology broached the idea of developing a subspecialty chest magnetic resonance imaging (MRI) practice over a year ago. We believed that MRI could provide soft tissue characterization and insights into noncardiovascular and nonmusculoskeletal chest pathology not otherwise attainable with traditional imaging of the chest such as radiographs, computed tomography (CT), and positron

emission tomography/computed tomography (PET/CT). We also believed that the historical stigma of MRI of the chest – largely related to MRI challenges in the setting of respiratory motion, cardiac motion, vascular pulsatility, air susceptibility, and simply the paucity of signal in the lung itself – could now be overcome by advances in hardware and pulse-sequence design techniques.

The literature on subspecialized chest MRI is relatively limited, although several groups have recently suggested clinical protocols.[1-7] Given the lack of prototype paradigms to follow, we needed to create our own. The purpose of this manuscript is to share our experience in developing a clinical chest MRI practice, highlighting insights gained and the protocols that worked well.

INITIATIVE

In most radiology practices, noncardiovascular, nonmusculoskeletal chest MRI is a relatively small niche with small clinical volumes. At our institution, a tertiary care academic center with a relatively large predominantly subspecialized MRI practice, 67,950 MRIs were performed between September 2011 and 2012, and of those, 218 (0.3%) were chest MRIs. Further parsing of the indications for these examinations revealed 11 that included the word "lung" or "pulmonary"; 5 with "mediastinal" or "mediastinum"; 9 with "brachial plexus"; and 16 with "chest wall" – approximately 41 cases in a year.

Traditionally at our institution, MRI of the chest wall and brachial plexus (for both posttraumatic and tumoral invasion) is handled by our musculoskeletal group, while the remaining noncardiovascular MRI cases are performed and interpreted by our abdominal group. When asked, our nonthoracic radiology colleagues were generally more than willing to give up the chest MRI cases because of conceded lesser expertise or interest. Even with collegial assent, creating a new practice requires a great deal of initiative particularly at large institutions with many administrative and leadership levels. Support by the Division Head of Thoracic Radiology is critical with much work done behind the scenes. Maintaining a position that the Division of Thoracic Radiology can provide subspecialty service to clinical colleagues and subspecialized care to the patient can be persuasive.

CLINICAL COLLABORATION AND READINESS

The main roadblocks to starting a chest MRI practice include: (1) the clinical perception that chest MRI should not be performed or is not useful, and (2) the lack of radiologist experience/expertise in this area. Conversations with our clinical colleagues from thoracic surgery, pulmonology,

medical oncology, radiation oncology, and thoracic pathology as well as participation at their tumor boards gave us opportunities to provide radiological insight into the role of MRI. Though not unanimous, the overwhelming majority were at least ready to consider chest MRI. In the Thoracic Radiology Division, radiologists with more than a passing interest in MRI were adequate to sustain this relatively small subspecialty practice. For us, starting a clinical chest MRI practice included a multidisciplinary research component to ascertain how well MRI evaluates chest pathology, and how well MRI demonstrates response to a therapy or helps in management. These investigations can spark niche applications as well as ultimately create the indications for MRI that will provide additional information for improved patient care.

The early stages of building a practice are rarely turn-key. Clinicians may get frustrated with the logistical challenges of ordering a chest MRI and may be overwhelmed by the increased number of images and the varied MR-specific information compared with the more familiar CT examination. It is also easy to forget the longer examination times; a CT may take 5 min while an MRI examination can range from 15 to 60 min depending on the anatomic and functional scope of the examination. Having a point-radiologist helps to address all these matters.

ALLIED HEALTH AND SUPPORT

The MRI technologists who acquire our chest MRI examinations are a mixed group of body, neuro, and "general" MRI technologists; they all share the same interest, enthusiasm, drive, and ability to think on their feet. This is particularly important, as patient-related limitations not unique to chest MRI such as dyspnea, poor breath-holding capacity, or inability to lie supine can compound the inherent challenges of MRI of the chest.

Workflow is largely protocol-driven at our institution. Triaging orders, and scheduling chest MRIs differently from other body MRIs are not always straightforward, particularly if the purpose is to ensure that the MRI gets protocoled and read by the appropriate radiologist. Our departmental nurses also use protocols for intravenous contrast requests. In the early phases of developing a practice when there may be no protocol in place, it is again helpful to provide these groups with a contact radiologist in the Thoracic Division to assist.

SCANNER CONSIDERATIONS AND SCANNER TIME

In our clinical practice, we have two MRI platform vendors, Siemens (Siemens Healthcare, Erlangen, Germany) and

GE (GE Healthcare, Waukesha, WI). For the most part, there is nothing significantly different between pulse sequences that one would choose to use in a diagnostic protocol from one vendor to the next. As published, chest MRI protocol suggestions have been developed on Siemens platforms[1-7] and are available as standard protocols on Siemens scanners (Syngo B17, Siemens Healthcare, Erlangen, Germany); we began our efforts by evaluating the performance of the proposed sequence protocols. At our institution, the Siemens platform is almost exclusively used for neuroimaging. This required discussions at several leadership levels to request and coordinate time on the Siemens scanners. As the body MRI practice at our institution is almost exclusively performed on GE platforms, we soon began efforts to optimize a chest MRI protocol on this platform to ensure long-range patient access and practice sustainability. Ultimately, the goal is to obtain the highest quality diagnostic examination and answer the clinical question for each patient, regardless of vendor.

PROTOCOL DEVELOPMENT

Thanks to investigators in Germany, a "thoracic" protocol is readily available in the Siemens User Tree on their 1.5T Siemens platforms (Syngo B17, Siemens Healthcare, Erlangen, Germany);[1-7] these references also provide generic pulse sequences portable across vendors. In this section, we discuss some of the developments in this area as well as optimizations and modifications to the suggested protocols that seem to have served us well so far. Optimizations were initially performed on phantoms, and this proceeded to scanning normal volunteers. It is critical that preliminary scanning includes several normal volunteers, as only then can one truly appreciate the nuances of respiratory triggering, navigator triggering, and even breath-holding, all critical components that need to be addressed.

For all examinations, a receive-only phased-array surface coil is placed over the chest, making sure that coverage is adequate; this may require two surface coils. When more coil coverage is needed, it is often considered in the craniocaudad dimension, but also realize that more coil coverage may be helpful along the lateral aspects of the chest, particularly in larger patients with relatively large anterior–posterior dimensions. Coil coverage may also need to be adapted based on the particular clinical question. A sensor for respiratory-triggered acquisitions is also positioned at the start of each examination.

Unless there is a contraindication for gadolinium-based intravenous contrast, our patients will get an 18G needle access that will support power injection of contrast at a rate of 3 cc/s. If contrast is administered, we use 80% or less of a single dose (0.1 mmol/kg) of gadobenate dimeglumine.

Each acquisition series is detailed below, with particular attention paid to describing modifications and optimizations to sequences, which we found helpful, nuances of executing the protocol, and the rationale for using a particular sequence. Additional parameters are detailed in Tables 1 and 2.

Series 1: Scout

The scout is acquired as a free-breathing half-Fourier acquired single-shot turbo spin echo (Siemens HASTE) or single-shot fast spin echo technique (GE SSFSE). During this 25-s scan, 28 slices are acquired: 8 in the sagittal plane, 5 in the coronal plane, and 15 in the axial plane.

Series 2: Coronal T2 breath-held

In addition to its role as a screen for pathology, this series can be used as a reference for prescribing subsequent breath-held sequences. HASTE or SSFSE is typically the default sequence, allowing complete chest coverage in a single breath-hold. If further detail is desired, a 2D multislice multibreath-hold turbo spin echo (Siemens TSE) or fast spin echo (GE FSE) can be employed. We currently use a periodically rotated overlapping parallel lines with enhanced reconstruction (PROPELLER) technique acquired in about 5-6 breath-holds of about 17-23 s. BLADE is the Siemens proprietary variant of PROPELLER. We have found that the central k-space oversampling and inherent motion correction properties of this technique result in less motion artifact from the heart and subtle respiratory modulations as well as increased sharpness of the lung/pleural interface. Analogous observations in the pelvis have been reported.[8] Radial artifacts can be minimized by appropriate attention to blade width and oversampling parameters.

Series 3: Coronal 2D bSSFP, free-breathing

This series is a nonfat-saturated 2D multislice balanced steady state free precession (bSSFP) sequence. These image acquisitions are often extremely useful, providing exquisite anatomic information and soft tissue contrast as well as dynamic information on diaphragmatic excursion with respiration. Occasionally, relative tumor mobility can be assessed on these image acquisitions. This 2D technique of evaluating lung motion in both healthy volunteers and in patients with intra- and extra-pulmonary disease has been compared with other investigational 3D MRI techniques[9] with reported good correlation. In patients who cannot receive intravenous gadolinium, bSSFP images often provide an adequate look at the central vascularity.

Table 1: Chest MRI scanning parameters on a siemens 1.5T magnet

Series no.	Series description	Resp. tech.	Siemens							
			Pulse sequence	FOV (cm)	Matrix size (ph × freq)	Slice thick. (mm)	TR/TE (ms/ms)	No. of slices	BW (Hz/Px)	Other parameters
1	Scout	FB	HASTE	44	192 × 256	8	900/84	8 sag; 5 cor; 15 ax	407	-
2	Coronal T2	BH	BLADE TSE	36	256 × 256	5	3000/171	30	501	BLADE coverage = 120% Turbo factor = 71 IPAT = 2 Concatenations = 5
3	Coronal 2D bSSFP	FB	TRUE FISP	42	256 × 256	4 with −60% gap	415/1.16	128	1028	Single shot
4	Navigator scout	FB	HASTE	44	192 × 256	8	900/84	15 cor; 9 ax	407	-
5	Axial T2	NT	BLADE TSE	36	320 × 320	5.5	var/96	41	300	Turbo factor = 30 BLADE coverage = 200%
6	Axial DWI	RT	EPSE	38	160 × 160	5.5	var/81	41	2084	Averages = 4 IPAT = 2
7	Pregadolinium T1 3D SPGR	BH	Dixon VIBE with CAIPARINHA	34	162 × 288	3.3	6.09/2.339/ (TE$_2$ 4.78)	var	300/1020	Flip angle = 12 Acceleration = 4
8	Test Bolus	FB	FLASH GRE	40	197 × 256	18	35.08/1.43 (min TR/min TE)	1	400	-
9	Postgadolinium T1 3D SPGR	BH	Dixon VIBE with CAIPARINHA	34	162 × 288	3.3	6.09/2.339/ (TE$_2$ 4.78)	var	300/1020	Flip angle = 12 Acceleration = 4
10 (opt)	T1 SPGR In-and out-of-phase	BH	(From series 7)							
11 (opt)	Axial bSSFP	BH	TRUE FISP	38	204 × 256	5 skip 1	(Parameter optimization still under investigation)			
12 (opt)	Cine bSSFP	FB	TRUE FISP	42	256 × 256	4	415/1.16	1	1028	Single shot

FOV: Field of view, TR: Repetition time, TE: Echo time, BW: Bandwidth, FB: Free-breathing, RT: Respiratory-triggered, NT: Navigator-triggered, ph: Phase, freq: Frequency, Px: Pixel, sag: Sagittal, cor: Coronal, ax: Axial, Thick: Thickness, Resp. Tech: Respiration technique, opt: Optional, Ph Accel: Phase acceleration, var: Variable, BH: Breath hold

Table 2: Chest MRI scanning parameters on a GE 1.5T magnet

Series no.	Series description	Resp. tech.	GE							
			Pulse sequence	FOV (cm)	Matrix size (freq × ph)	Slice thick. (mm)	TR/TE (ms/ms)	No. of slices	BW (Hz)	Other parameters
1	Scout	FB	SSFSE	48	352 × 192	10		15 ax 7 sag 11 cor	62.50	-
2	Coronal T2	BH	FRFSE	40	256 × 256	6, skip 1	2250/102	32	50	ETL = 19
3	Coronal 2D bSSFP	FB	2D FIESTA	40	192 × 256	4, skip 2	3.5/min TE	118	100	-
4	Axial T2	RT	PROPELLER FSE	38	320	5, skip 1	var/101	20	125	ETL = 32 Nex = 3 Refocus angle = 160 PhAccel = 3
5	Axial DWI	RT	EPI	38	128 × 128	6, skip 1	min TE	27	83.33	-
6	Pregadolinium T1 3D SPGR	BH	LAVA-Flex with ARC	35	320 × 224	4	6.6/min TE	60	83.33	Flip angle = 12
7	Test bolus	FB	GRE	40	256 × 128	6	13.7/min TE	1	62.5	-
8	Postgadolinium T1 3D SPGR	BH	LAVA-Flex with ARC	35	320 × 224	4	6.6/min TE	60	83.33	Flip angle = 12
9 (opt)	T1 SPGR in-and out-of-phase	BH	SPGR	40	256 × 192	5, skip 1	140/2.1/ (TE$_2$ 4.4)	var	62.5	Flip angle = 70
10 (opt)	Axial bSSFP	BH	2D FIESTA	40	192 × 256	5, skip 2	3.5/1.2	var	125	-
11 (opt)	Cine bSSFP	FB	2D FIESTA	40	192 × 224	5, skip 2	3.5/1.2	1	125	-

FOV: Field of view, TR: Repetition time, TE: Echo time, BW: Bandwidth, FB: Free-breathing, RT: Respiratory-triggered, NT: Navigator-triggered, ph: Phase, freq: Frequency, Px: Pixel, sag: Sagittal, cor: Coronal, ax: Axial, Thick: Thickness, Resp. Tech: Respiration technique, opt: Optional, Ph Accel: Phase acceleration, var: Variable, BH: Breath hold

Series 4: Navigator scout

The purpose of this series is to optimize placement of a 2D navigator for subsequent navigator-triggered acquisitions. Navigator Scout images are HASTE/SSFSE acquisitions, which, at first glance, may seem like a redundant series to the Scout Series. We have observed that: (1) initial anxiety can lead to erratic diaphragmatic motion, which is generally allayed this far into the examination, making tracking of the right hemi-diaphragm more regular at this point of the examination, and (2) we can obtain a more reliable location of the posterior aspect of the dome of the liver on an axial slice, which is an optimal place for navigator placement. Some patients who have had surgery on the right side may have suboptimal right hemi-diaphragmatic excursion, and in those instances, we have been successful in placing the navigator on the left hemi-diaphragm at the level of the spleen.

Series 5: Axial T2 navigator-triggered

We have found T2 TSE BLADE/PROPELLER to be qualitatively comparable to, if not favored over, conventional T2 TSE acquisitions, particularly given the reduced sensitivity to cardiac motion and increased sharpness of the major tissue interfaces. Fat saturation is routinely employed for this series. In addition to lesion characterization, this sequence is highly useful for the evaluation of lymphadenopathy and regional bone marrow signal.

Series 6: Axial diffusion-weighted imaging, respiratory-triggered

For this 2D multislice echo planar imaging (EPI) respiratory-triggered acquisition, we have selected b values of 0, 100, and 800 s/mm^2. Diffusion-weighted imaging (DWI) in other body systems has provided information suggesting the cellularity of the lesion of interest and, because of this, is of particular interest as a potential biomarker of disease and treatment response. To obviate any T2* effects that could be induced in the lesion due to gadolinium, we have decided to perform DWI prior to contrast administration. Further investigation is needed to determine if "pseudoperfusion" (intravoxel incoherent motion) effects elucidated by using lower b-values (less than 100 s/mm^2) provide additional clinically relevant information.

Series 7: Pregadolinium T1 3D SPGR

A variety of 3D T1-weighted fat-saturated gradient recalled echo (GRE) sequences are available. Currently, we use a 3D spoiled gradient recalled (SPGR) with accelerated parallel imaging acquisition technique (Siemens VIBE with CAIPIRINHA or GE LAVA-Flex with Auto-calibrating Reconstruction for Cartesian (ARC) sampling and Dixon method for fat suppression, repition time/echo time TR/TE (3.82/1.8 ms), and matrix/slice thickness (256 × 256)/3 mm. In- and -out-of-phase images are routinely reconstructed. Homogeneous fat saturation of the anterior-superior mediastinum near the origin of the great vessels can be challenging with non-Dixon methods and particular attention to manual shim boxes is helpful in this regard.

Series 8: Test bolus

For this portion, repeated real-time single-slice GRE axial acquisitions at the level of the pulmonary artery are acquired following injection of 1 cc of intravenous contrast followed by a 20 cc normal saline flush. The time to peak enhancement in the pulmonary artery or ascending aorta can be determined.

Series 9: Postgadolinium T1 3D SPGR

Using the information from the test bolus, the initial postgadolinium series is timed such that peak arterial enhancement coincides with the time of central k-space filling. Identical parameters are used for the pre- and postgadolinium series, with images typically acquired in the axial plane. Subsequent postgadolinium images are typically obtained at 1, 3, and around 5 min. An additional imaging plane, either coronal or sagittal, is often obtained.

Series 10 (optional): T1 SPGR breath-held In- and out-of-phase

The information provided by this dual-echo 2D GRE sequence with respect to the presence of intravoxel fat is particularly useful in imaging anterior mediastinal masses where the normal or hyperplastic thymus is a consideration.[10] The imaging parameters are Repetition Time/First Echo Time/Second Echo Time (TR/TE^1/TE^2) (170/2.38/4.76 ms), matrix/slice thickness (256 × 192)/5.5 mm. In practice, we have found the in- and out-of-phase images obtained from the pregadolinium T1 3D SPGR with Dixon technique can be comparably used, thus saving the time associated with running a separate two-dimensional T1-weighted Gradient-Recalled Echo (2D T1 GRE) for this purpose.

Series 11 (optional): Axial bSSFP breath-held

The 2D bSSFP (Siemens TRUE FISP or GE FIESTA) technique demonstrates T2/T1-weighting with high contrast and signal-to-noise ratio and can be obtained with rapid sequential acquisition, fat suppression, and overlapping thin sections. It is frequently used in cardiac and abdominopelvic MRI as a noncontrast-enhanced bright blood MR angiography/venography technique. These are typically performed as breath-held acquisitions but can be tailored to be free-breathing.

Series 12 (optional): Cine bSSFP

Cine bSSFP (Siemens TRUE FISP or GE FIESTA) is a staple of cardiac imaging for the evaluation of cardiac wall motion, function, and valves. In the context of noncardiac chest MRI, this technique is useful for evaluating the motion of an intrapulmonary mass relative to the mediastinum or chest wall in assessing for possible invasion.

We have found that the above sequences and modifications provide a robust set of tools to draw upon in answering most clinical questions. As always, a specific examination may require additional considerations, such as ECG-gating or an angiographic technique. It is becoming increasingly common for facilities to have default protocols and radiologists sitting in the reading room at a remote site. We believe it is important for the radiologist to evaluate the quality of the scan while the patient is still on the scanner as there are several opportunities to optimize or shorten the scan right at the console. Shortening the scan

time can be particularly important for patients who are dyspneic, anxious, or who have trouble lying supine for a prolonged time, all fairly common occurrences in our patient population.

RADIOLOGY ECONOMICS

Regarding cost, the nominal fee of an MRI without and with contrast costs almost twice as much as a CT without and with contrast, and the Medicare fee (in the United States) for an MRI costs about 1.7 times as much as a comparable CT. In terms of relative value units (RVU, a metric in the United States designed to measure physicians' work activity in uniform units), the only comparison available is a nonspecified chest MRI with and without contrast that generates roughly 10 times the RVUs for a chest X-ray and about 1.6 times that for a chest CT. Higher reimbursement for MRI is probably related to a number of factors, including initial cost of the equipment, maintenance, and patient throughput; however, the examination time for an individual patient does not affect the cost of the examination, since the length of the time slots are predetermined. We do believe that examinations should be as short as possible, particularly in a patient population that may have limited tolerance for long breath-holds or even lying supine for an extended period.

CASES

In many cases, the exquisite soft tissue detail from MRI provides great benefit in guiding clinical decision-making and patient management [Figures 1-5].

Case 1

A 32-year-old male with biopsy-proven sarcomatoid carcinoma involving the right middle lobe was evaluated by MRI. Figure 1 shows an example of the right middle lobe malignant mass suspicious of pericardial invasion, a finding confirmed at surgery. In this case, T2-weighted images using a BLADE TSE/PROPELLER FSE technique and ECG-gated double inversion-recovery FSE images were particularly useful in characterizing disease extent.

Case 2

A 25-year-old female with chromosomal abnormality, and severe combined pectus excavatum and carinatum deformity presented with a large mediastinal mass. T2-weighted and contrast-enhanced T1-weighted images illustrate the exquisite soft tissue contrast, detail, and extent of a complicated cystic mass consistent with lymphatic malformation [Figure 2].

Case 3

A 45-year-old female with chronic upper respiratory symptoms and dry cough had an MRI as part of her imaging

work-up. Contrasting soft tissue signaling features in the mediastinum can be particularly improved with some MRI techniques such as DWI [Figure 3] as shown in this case. Based on the imaging features differential considerations included thymoma and left phrenic nerve sheath tumor. Surgery followed with pathology indicating a thymoma with extensive cystic change.

Case 4

A 53-year-old male with a large left hemithorax mass could not tolerate lying supine in the MRI scanner, and the entire study was performed with the patient in the left lateral
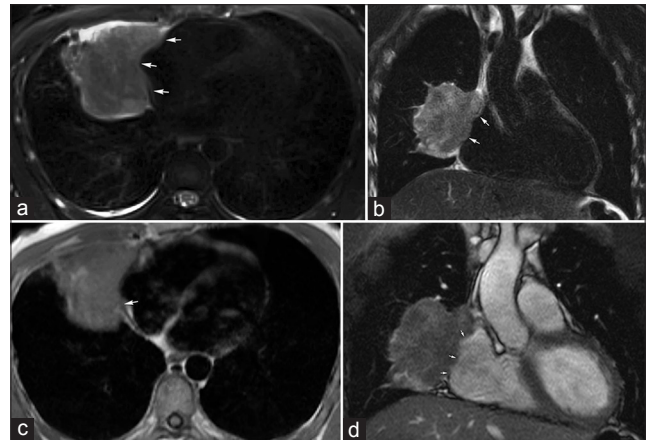

Figure 1: 32-year-old male with biopsy-proven sarcomatoid carcinoma involving the right middle lobe. MRI was performed to evaluate disease extent. (a) Axial and (b) coronal T2-weighted images using a PROPELLER/BLADE technique demonstrate the lobulated right middle lobe mass invading the mediastinal fat medially (arrows). (c) Gated double inversion-recovery FSE "black-blood" image shows the loss of the hypotense pericardial line (arrow), and (d) real-time free-breathing bSSFP image shows lack of apparent separation (arrows) highly suspicious for pericardial invasion, a finding confirmed at surgery.
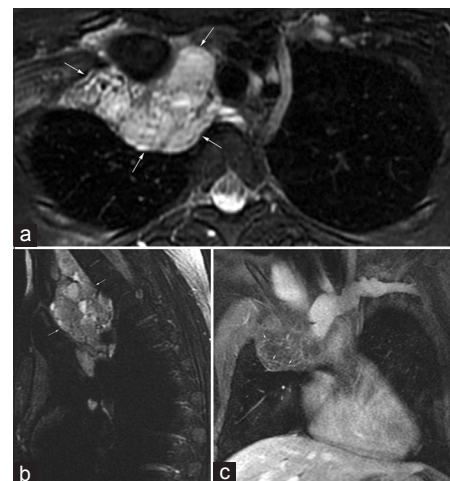

Figure 2: 25-year-old female with chromosomal abnormality, mediastinal mass, and severe combined pectus excavatum and carinatum deformity. (a) Axial and (b) sagittal T2-weighted images demonstrate a multilobulated, multiseptated cystic mass (arrows) with multiple fluid-fluid levels in the right side of the superior mediastinum extending into the right side of the neck and to the junction of the superior vena cava and the right atrium. (c) Coronal postcontrast T1-weighted image demonstrates thin septal enhancement (arrows). Findings are consistent with a large lymphatic malformation for which the patient had previously undergone surgery.
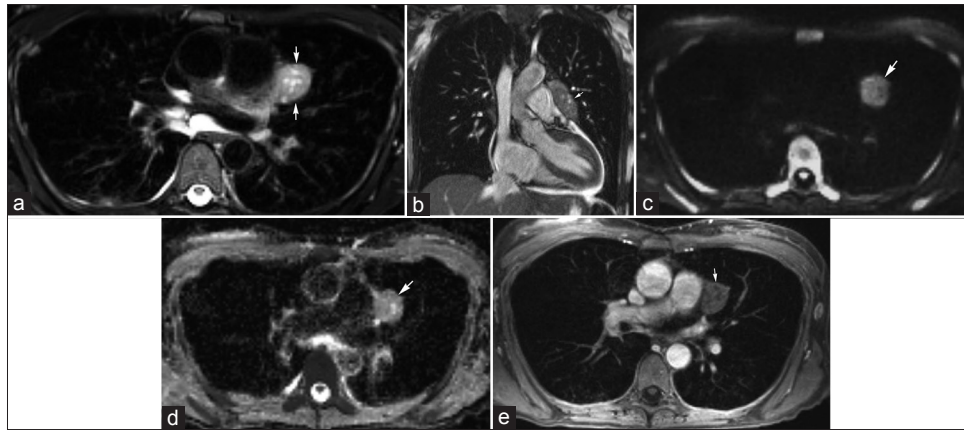
Figure 3: A 45-year-old female with chronic upper respiratory symptoms and dry cough. (a) Axial T2-weighted image and (b) coronal bSSFP image demonstrate an elongated rounded mass (arrows) with internal cystic areas along the course of the left phrenic nerve. (c) Diffusion-weighted image using b=800 s/mm^2 and correlating (d) apparent diffusion coefficient (ADC) map show no appreciable restricted diffusion (arrow). (e) Contrast-enhanced axial image demonstrates minimal enhancement of this mass (arrow). Differential considerations include thymoma and left phrenic nerve sheath tumor. The mass was resected with pathology indicating a thymoma with extensive cystic change.
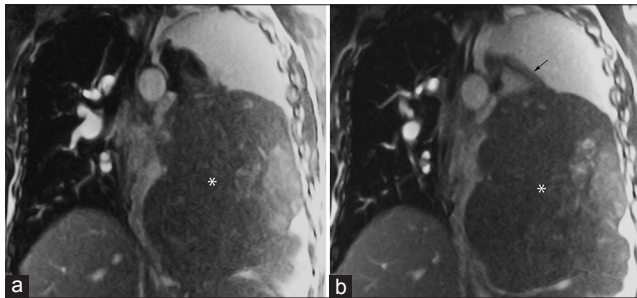

Figure 4: 53-year-old male with a large left hemithorax mass. (a and b) Coronal noncontrast-enhanced real-time free-breathing bSSFP images demonstrate a large extra-pulmonary mass (*) that arises from the left inferior pulmonary ligament (arrow). Differential considerations include sarcoma or fibrous tumor of the pleura. This was surgically excised with pathology indicating solitary fibrous tumor with focal tumoral necrosis.

decubitus position. For patients who cannot lie supine or who are severely short of breath, noncontrast-enhanced fast imaging techniques such as bSSFP can provide helpful information [Figure 4]. Differential considerations included sarcoma or fibrous tumor of the pleura. The mass was surgically excised with pathology indicating solitary fibrous tumor with focal tumoral necrosis.

Case 5

An 85-year-old male with malignant mesothelioma presented with focal right-sided anterior pain. Staging of mesothelioma by CT and PET/CT may benefit from improved soft tissue contrast provided by MRI particularly along the mediastinal pleura [Figure 5]. The region of focal pain corresponded to a mass, which demonstrated restricted diffusion.

CONCLUSION

Noncardiovascular nonmusculoskeletal chest MRI is at the optimal time for implementation, and several topics
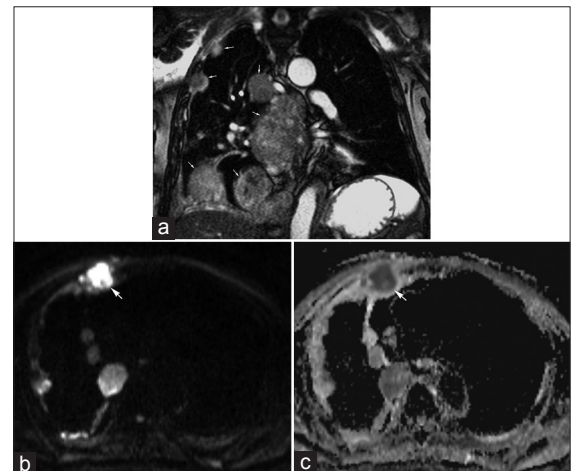

Figure 5: 85-year-old male with malignant mesothelioma having focal right-sided anterior pain. (a) Coronal real-time free-breathing bSSFP image illustrates multiple pleural masses (arrows) consistent with known malignant mesothelioma. (b) Diffusion-weighted image using b=800 s/mm^2 and corresponding (c) apparent diffusion coefficient (ADC) map demonstrate restricted diffusion in one of the pleural masses (arrow). The location of this mass corresponded with the region of focal pain.

discussed here help to provide practical steps and insight to developing a thriving chest MRI practice. With appropriate teams and protocols in place, the complications of chest MRI imaging can be overcome to provide the diagnostic imaging quality of soft tissue detail that can make a difference in clinical decision making and patient management.

ACKNOWLEDGMENTS

REFERENCES

1. Biederer J, Beer M, Hirsch W, Wild J, Fabel M, Puderbach M, et al. MRI of the lung (2/3). Why ... when ... how? Insights Imaging 2012;3:355-71.
2. Biederer J, Hintze C, Fabel M, Jakob P, Horger W, Graessner J, et al. MRI of the Lung – ready … get set … go! Magnetom Flash 2011;1:6-14.
3. Biederer J, Mirsadraee S, Beer M, Molinari F, Hintze C, Bauman G, et al. MRI of the lung (3/3)-current applications and future perspectives. Insights Imaging 2012;3:373-86.
4. Biederer J, Puderbach M, Hintze C. A Practical Approach to Lung MRI at 1.5T. Magnetom Flash 2006;238-43.
5. Puderbach M, Hintze C, Ley S, Eichinger M, Kauczor HU, Biederer J. MR imaging of the chest: A practical approach at 1.5T. Eur J Radiol 2007;64:345-55.
6. Wielputz M, Kauczor HU. MRI of the lung: State of the art. Diagn Interv Radiol 2012;18:344-53.
7. Wild JM, Marshall H, Bock M, Schad LR, Jakob PM, Puderbach M, et al. MRI of the lung (1/3): Methods. Insights Imaging 2012;3:345-53.
8. Lane BF, Vandermeer FQ, Oz RC, Irwin EW, McMillan AB, Wong-You-Cheong JJ. Comparison of sagittal T2-weighted BLADE and fast spin-echo MRI of the female pelvis for motion artifact and lesion detection. AJR Am J Roentgenol 2011;197:W307-13.
9. Plathow C, Schoebinger M, Herth F, Tuengerthal S, Meinzer HP, Kauczor HU. Estimation of pulmonary motion in healthy subjects and patients with intrathoracic tumors using 3D-dynamic MRI: Initial results. Korean J Radiol 2009;10:559-67.
10. Takahashi K, Inaoka T, Murakami N, Hirota H, Iwata K, Nagasawa K, et al. Characterization of the normal and hyperplastic thymus on chemical-shift MR imaging. AJR Am J Roentgenol 2003;180:1265-9.